PCCP

PAPER

View Article Online
View Journal | View Issue

Cite this: *Phys. Chem. Chem. Phys.*, 2022, **24**, 27380

Overlapping hydration shells in salt solutions causing non-monotonic Soret coefficients with varying concentration†

Shilpa Mohanakumar, [a] Hartmut Kriegs, [a] W. J. Briels [ab] and Simone Wiegand *[ac]

Received 2nd September 2022,
Accepted 28th October 2022

DOI: 10.1039/d2cp04089a

rsc.li/pccp

We investigate the thermodiffusive properties of aqueous solutions of sodium iodide, potassium iodide and lithium iodide, using thermal diffusion forced Rayleigh scattering in a concentration range of 0.5–4 mol kg^{-1} of solvent, large enough to deal with associated salts, and a temperature range of 15 to 45 °C. All systems exhibit non-monotonic variations of the Soret coefficient S_T with concentration, with a minimum at one mol kg^{-1} of solvent in all three cases. We take this as an indication that the relevant length and energy scales are very similar in all cases. On this basis we develop an intuitive picture in which the relevant objects are the fully hydrated salt molecules, including all water molecules that behave differently from bulk water. Preliminary, somewhat sketchy calculations indicate that indeed Soret coefficients begin to rise beyond concentrations where the fully hydrated particles are randomly close packed. Indications are given as to why the model will fail at large concentrations.

1 Introduction

Thermophoresis, also called thermodiffusion or Ludwig–Soret effect, describes mass transport in temperature gradients and is one of the interesting unsolved puzzles in physical chemistry. Nowadays the most prominent application of this effect is in the determination of binding constants in protein–ligand reactions,[1,2] but the effect also plays an important role in, for example, the conversion of waste heat into electricity by means of thermogalvanic cells.[3–5] In both cases a deeper understanding of thermodiffusion of ions in aqueous solutions is desirable. Since the pioneering work of Hofmeister, it is known that many physicochemical processes in aqueous salt solutions do not only depend on ion concentrations and valencies, but also on the ion type.[6–8] We therefore present experimental results of thermodiffusion in a range of concentrations and temperatures of solutions of three different salts with equal valencies but of different ion type, *in casu* lithium, sodium and potassium iodide.

In principle, in systems like ours there are four mass fluxes, *i.e.* those of the two types of ions, the one of the intact, non-dissociated salt molecules, and that of the solvent. Because of macroscopic electro-neutrality the two ionic fluxes must be equal. If we further assume that the dissociation equilibrium does not change with the very small temperature changes, the flux of the intact salt molecules must be equal to that of the individual ions. At the end we are left with only two independent mass fluxes, that of the solvent and that of the solute as a whole. From a phenomenological point of view we are therefore left with binary systems. From a microscopic point of view, the measured transport coefficients are combinations of those of the individual components.

In a binary fluid mixture exposed to a temperature gradient a stationary non-equilibrium state sets in, where the ordinary diffusive mass flux of the solute, proportional to the diffusion coefficient D, balances a thermophoretic mass flux of the solute, proportional to the thermal diffusion D_T. The Soret coefficient S_T defined as the ratio D_T/D describes the value of the concentration gradient that develops as a result of the applied temperature gradient. It can be positive, indicating that the solute accumulates in the cold region, or negative, in case the solute moves towards the warm region.[9,10] Especially in aqueous systems, variations of concentration or temperature may lead to sign changes and non-monotonous variations of S_T. While early studies of more than 20 different salts in water indicated monotonous behavior of the Soret coefficient with concentration,[11] later works reported a minimum of S_T for

[a] *IBI-4:Biomacromolecular Systems and Processes, Forschungszentrum Jülich GmbH, D-52428 Jülich, Germany. E-mail: s.wiegand@fz-juelich.de*
[b] *University of Twente, Computational Chemical Physics, Postbus 217, 7500 AE Enschede, The Netherlands. E-mail: w.j.briels@utwente.nl*
[c] *Chemistry Department – Physical Chemistry, University Cologne, D-50939 Cologne, Germany*

† Electronic supplementary information (ESI) available. See DOI: https://doi.org/10.1039/d2cp04089a

aqueous solutions of various salts.[12–14] A recent indication for a minimum of S_T with concentration was observed experimentally[15] and by computer simulations[16] for lithium chloride at very low temperatures. The simulations showed that the minimum disappeared with increasing temperature, and especially that artificially decreasing the size of the anion increased the depth of the minimum. Until now, all these phenomena are basically not understood on a microscopic level.[10,17–19]

According to Onsager's irreversible thermodynamics[20–22] the Soret coefficient S_T of a binary mixture may be written as

$$S_T = \frac{Q^*}{RT^2}\left(1 + \frac{\partial \ln \gamma_\pm}{\partial \ln c}\right)^{-1}, \quad (1)$$

where $\gamma_\pm$ is the activity coefficient of the salt and c the mass fraction of salt. Moreover, Q^* is an unknown quantity, containing both thermodynamic and kinetic contribution, and which is called the heat of transfer. Several expressions for Q^* have been suggested in the literature, some including kinetic contributions,[23] others ignoring them altogether.[17,24–26] The simplest of these models is the one of Prigogine,[17] who relates sign changes with concentration to a stronger cross interaction compared to the like–like interactions. This energetic concept works fine for many aqueous mixtures with ethanol,[27] saccharides,[28] methylformamides[29] and anionic surfactant sodiumdodecyl sulfate micelles in the presence of NaOH.[30] It also rationalizes the sign of the Soret coefficient in aqueous salt solutions at very low concentrations, *i.e.* below the dissociation limit.[14,15] In general, reasonable agreement may be found for non-polar mixtures, but all models fail for polar mixtures.[25] We have applied eqn (1), using the model of Kempers with thermodynamic data from several ref. 31–33 but have not been able to represent our results with any accuracy.

Variations of the Soret coefficient S_T with temperature often follow an empirical equation proposed by Iacopini and Piazza[34]

$$S_T(T) = S_T^\infty\left[1 - \exp\left(\frac{T^* - T}{T_0}\right)\right] \quad (2)$$

with obvious interpretations of the various adjustable parameters. In particular T^* is the temperature where the Soret coefficient changes sign, possibly outside the range of experimental data. Eqn (2) in particular does a good job with diluted aqueous solutions.[10,34,35] As we will see below, also S_T of halides follows this equation for all concentrations. This is not the case, however, for larger organic salts at low, and for non-ionic solutes at higher concentrations.[29,36–38]

Several computer simulation studies of thermodiffusion have appeared in the literature, some of which have been cited above, but none of these addresses salt solutions over a range of temperatures and concentrations. We will therefore not review these studies here in any detail. However, because we will refer to them on several occasions below, we do briefly discuss the results of thermophoretic simulations of binary Lennard-Jones mixtures by Artola and Rousseau.[39] All particles in their simulations were of equal mass and equal size. Simulations were performed over the full range of mole-fractions and a range of temperatures. Moreover they studied several different systems by varying like–like (ε_{AA}, ε_{BB}) and cross-interactions (ε_{AB}). Clearly, with Lennard-Jones energies $\varepsilon_{AA} = \varepsilon_{BB}$, and ε_{AB} such that component A goes to cold at small mole-fractions x_A, component B must go to cold at small mole-fractions x_B, *i.e.* at large mole-fractions x_A; as a consequence component A will go to hot at large mole-fractions x_A. The Soret coefficient of component A must therefore obey $S_T(x_A) = -S_T(1 - x_A)$, and change sign at $x_A = x_B = \frac{1}{2}$. From the simulations it follows that in all cases the Soret coefficient changes linearly with mole-fraction, and indeed obeys the rule just mentioned. Moreover, it was found that changing k_{AB} in $\varepsilon_{AB} = k_{AB}\sqrt{\varepsilon_{AA}\varepsilon_{BB}}$ changes the slope of this line, while varying the ratio $\psi = \varepsilon_{BB}/\varepsilon_{AA}$ induces a vertical (or horizontal if you prefer) shift of the line. Before ending this paragraph on computer simulations we mention one more study on Lennard-Jones mixtures by Bresme *et al.*,[40] where the authors perform in depth calculations of all properties of their mixtures relevant for testing several theories proposed to describe Soret coefficients so far. Their calculations are restricted however to one particular set of Lennard-Jones parameters, and therefore cannot be used for our purposes (see below).

Even when no theoretical explanation for the occurrence of a minimum in the Soret coefficient with variations of concentration is available, some hypotheses/speculations concerning the origin of the phenomenon may be found in the literature. Chanu,[13] and later Gaeta *et al.*[14] pointed at the perturbation of local order of water in the neighborhood of the ions and its dependence on salt concentration as a possible starting point for an understanding of the non-monotonous dependence of Soret. This picture of perturbed water goes back to Frank and Wen.[41] Evidently, in dense solutions, solvent molecules must organize their structure in order to accommodate to the presence of the solutes. Indeed, strong variations of water densities around NaI, among other salts, have been confirmed in a paper by simulations and neutron diffraction experiments[42–46] and around CO_2 by Mitev *et al.*[47] A closer look at the structure in the latter case reveals that water molecules very close to the solute are strongly bound to that solute, either by expressing their negative oxygen atom to the slightly positive carbon atom on CO_2, or by embracing the slightly negative oxygen atom on CO_2 with their hydrogen atoms. Similar structures may be assumed to occur around dissolved salt molecules. Beyond this first shell of water molecules, a second shell of decreasingly perturbed water molecules is needed to gradually adjust to bulk water. As a result, the CO_2 molecule plus perturbed water is roughly a sphere with a radius of about 6–7 Å.[47]

In this paper we will adopt a similar picture for salt solutions. For simplicity we assume that the measured effective transport coefficients may be attributed to non-dissociated salt molecules. Further discussion of this assumption will be given in Section 3.1. We define three types of particles, the bare salt molecule consisting of a cation paired with an iodide ion, the hydrated salt molecule (HSP) consisting of a bare salt molecule

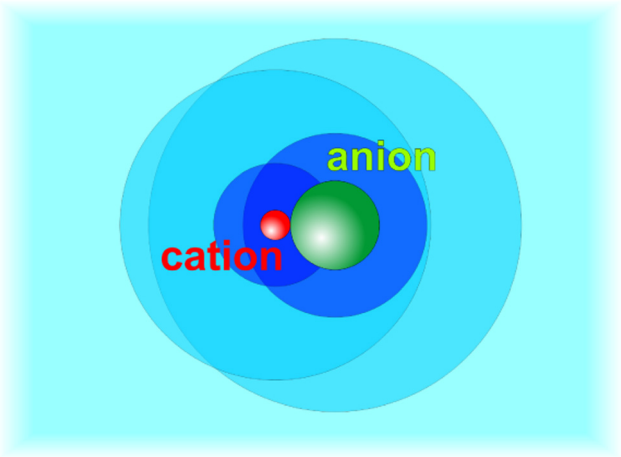

Fig. 1 Model of a hydrated salt molecule with a first shell of tightly bound water molecules (dark blue and a second shell of perturbed water (light blue). For simplicity the molecule including the two hydration shells will be assumed spherical.

plus a first layer of Z strongly bound solvent molecules, and the fully hydrated salt molecule (FHP) consisting of the hydrated salt molecule plus the shell of perturbed water molecules. A caricaturist picture of these definitions is shown in Fig. 1. We expect that the Soret coefficient will change monotonously with concentration up to random close packing of the FHPs, beyond which the behavior will change. Random close packing occurs at a volume fraction of $\phi = 0.64$,[48] which with a radius of 6–7 Å corresponds to a molality of about 1.0 mole of salt per kilogram of water. This indeed turns out to roughly coincide with the minimum of Soret in all systems that we studied. We will use this observation as the starting point of our analysis of the thermophoresis of salt solutions with molalities on the order of one mole kg^{-1} of water.

2 Results

2.1 Concentration dependence

We used Infrared Thermal Diffusion Forced Rayleigh Scattering (IR-TDFRS) to investigate the thermophoretic behavior quantitatively. A schematic diagram of the setup is discussed in ESI† (Section S1) By way of example, we present in Fig. 2 the diffusion coefficient D, the thermal diffusion coefficient D_T, and the Soret coefficient S_T of NaI at four different temperatures as function of concentration. The solid lines are guides to the eye. As a measure of concentration we use molality m, *i.e.* the number of moles of salt per kilogram of water. At all temperatures D_T shows a minimum around a molality of 1 mol kg^{-1}, which survives in S_T, only slightly smoothed by increasing D. In all cases the diffusion coefficient D increases monotonously with concentrations, with the increase at higher concentrations being less than that at lower concentrations, due to an increase of viscosity with increasing salt concentration.[49] At the lowest measured temperature S_T and D_T change sign twice with concentration. Around m = 1 mol kg^{-1} NaI is

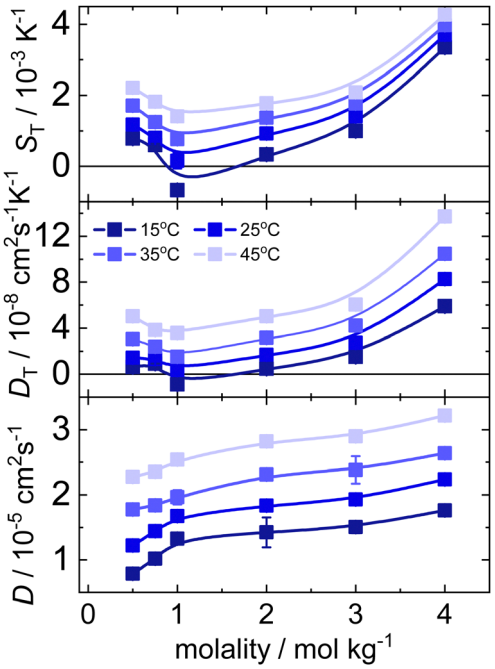

Fig. 2 Concentration dependence of Soret coefficient S_T, thermodiffusion coefficient D_T and diffusion coefficient D of NaI at four different temperatures as indicated in the inset. The lines are guides to the eye.

thermophilic (goes to hot), while at lower and higher concentrations it reveals thermophobic behavior (goes to cold). Potassium and lithium iodide behave similarly, but none of them shows a double sign change (*cf.* Fig. S4 and S5, ESI†).

Fig. 3 displays the concentration dependence of S_T values at 25 °C of the three iodide salts that have been studied. The lines are guide to the eye. All S_T of the investigated systems show a minimum with concentration, around 1 mol kg^{-1}, as has been observed for several other electrolytes.[13–15,38] The concentration at which the minimum is observed varies only marginally for different salt systems. The steepest decay at low concentrations is found for LiI, which is the most hydrophilic of the investigated systems.

2.2 Temperature dependence

Fig. 4 shows the measured S_T as function of temperature at a molality of 1 and 4 mol kg^{-1}. The curves have been fitted using eqn (2). The Soret coefficient shows an increase with increasing temperature for all salt systems investigated, which is typical for aqueous solutions at low concentrations. At 1 mol kg^{-1} S_T of KI and NaI show a sign change with temperature (*cf.* Fig. 4a), while LiI, as expected from the previous literature, shows thermophilic behavior at all concentrations.[50] Additionally, S_T of LiI remains almost constant with increasing concentration, while the thermophobicity of the other salts increases with concentration.

In a previous investigation where S_T of a number of electrolytes had been studied at 0.01 mol kg^{-1} of water, Snowden and Turner[51] found at 25.3 °C the largest negative value of S_T for LiI, -1.44×10^{-3} K^{-1}. Also, in our study LiI exhibits large negative

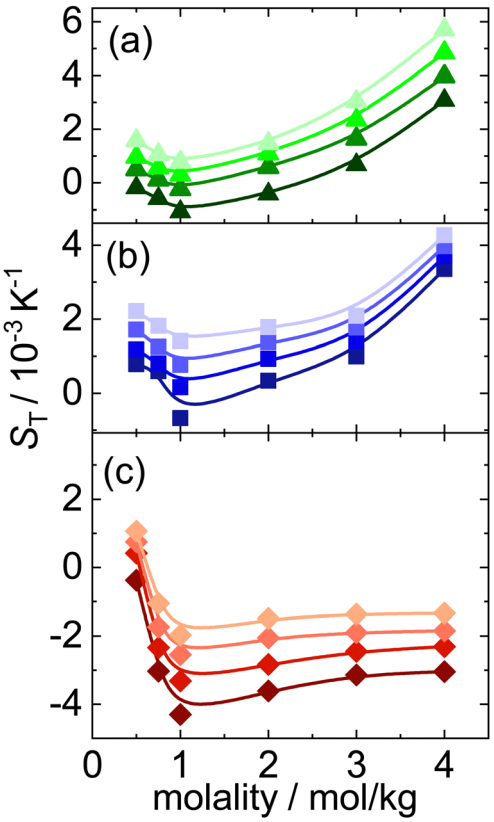

Fig. 3 Concentration dependence of Soret coefficient S_T of KI (upper panel), NaI (middle panel) and LiI (lower panel) at all measured temperatures. In each panel temperatures are 15, 25, 35 and 45 °C in that order, with the lowest temperature corresponding to the darkest set of symbols. Lines are guides to the eye.

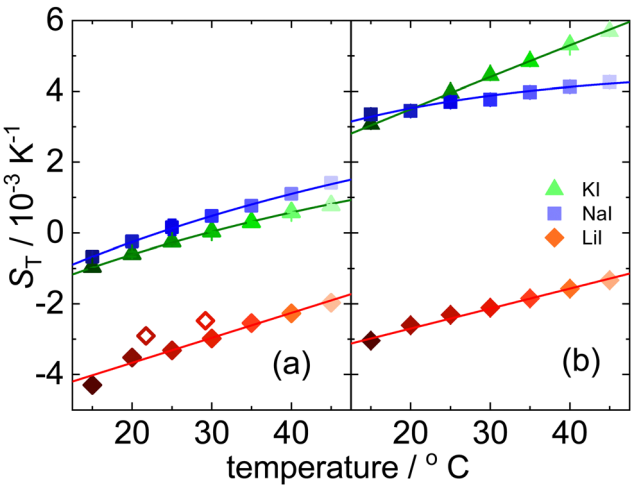

Fig. 4 Temperature dependence of Soret coefficient S_T of KI, NaI and LiI at molalities of 1 (left panel) and 4 (right panel) mol kg^{-1} respectively. The open symbols mark data points by Caldwell.[50] Darkest symbol corresponds to the lowest temperature of 15 °C with gradually fading to lighter symbols towards higher temperatures.

S_T values in comparison to KI and NaI (*cf.* Fig. 4). In a previous study of LiI Caldwell *et al.*[50] reported a S_T value of -2.69×10^{-3} K^{-1}, while we found an 11% lower value of -3.01×10^{-3} K^{-1} under the same conditions.

Fig. S6, S7 and S8 in the ESI,† display the temperature dependence of D_T and D. Both D_T and D show an increase with temperature. The increase in D is associated with the decrease in viscosity with temperature.

3 Discussion

3.1 Concentration dependence

In this section we infer from the characteristics of the data presented above a coarse grain picture that, in our view, contains the relevant elements to model the physics of our systems. In the second part we present results from some quick, but rather incomplete calculations on the basis of this model.

3.1.1 Rationalizing the results. Two things immediately stand out in all plots of Soret coefficients in Fig. 3. First, the data at low concentrations roughly depend linearly on concentration, with the slope being pretty constant for all systems and all temperatures. Second, the concentration where the minimum occurs varies only marginally among the different salts. The first observation agrees with the findings of Artola and Rousseau discussed in Section 1, while the second is consistent with the assumption that, at least at low concentrations, all salt molecules behave like equally big spherical particles.

It is known that in all cases that we consider about 80% of the salt molecules are dissociated into independent ions, while only 20% of them exist as non-dissociated, intact salt molecules.[52–54] We notice, however, that also among the dissociated ions the cation–anion pair correlation functions have very strong first peaks, mainly as a result of the strong Coulomb interactions. In agreement with the second of the above findings we therefore assume that on average we may treat the salt molecules as single particles, sometimes consisting of strongly bound ion pairs, sometimes consisting of more loosely bound ion pairs, and sometimes even as single anions. A particle like this is called a bare salt molecule from now on. The properties attributed to such a bare salt molecule must be considered to be effective properties, very much as discussed in Section 1. Clearly, the model that we describe below will become less applicable with increasing cation sizes. If needed, a more realistic, but also more complicated model may be devised along similar lines. Referring to Fig. 1, we recall the definition of hydrated salt molecule (HSP), consisting of a bare salt molecule plus the first layer of strongly attached water molecules, and the fully hydrated salt molecule (FHP), consisting of an HSP plus the layer of perturbed water molecules. The radius of such an FHP will be denoted R_{HS}. We obtain an estimate of this radius by assuming that the FHPs are randomly close packed when the molality is equal to m_{min}. The volume fraction of FHPs ϕ is given as

$$\phi = \frac{N_s V_{HS}}{V} = N_{Av} \frac{\rho m}{m_0 M_w + m M_s} V_{HS} = N_{Av} \mathscr{M} V_{HS}, \qquad (3)$$

where m is the molality of the solution, m_0 is the molality of water, *i.e.* the number of water molecules in one kilogram of water, M_s and M_w are the molar masses of salt and water respectively, and $\mathscr{M}$

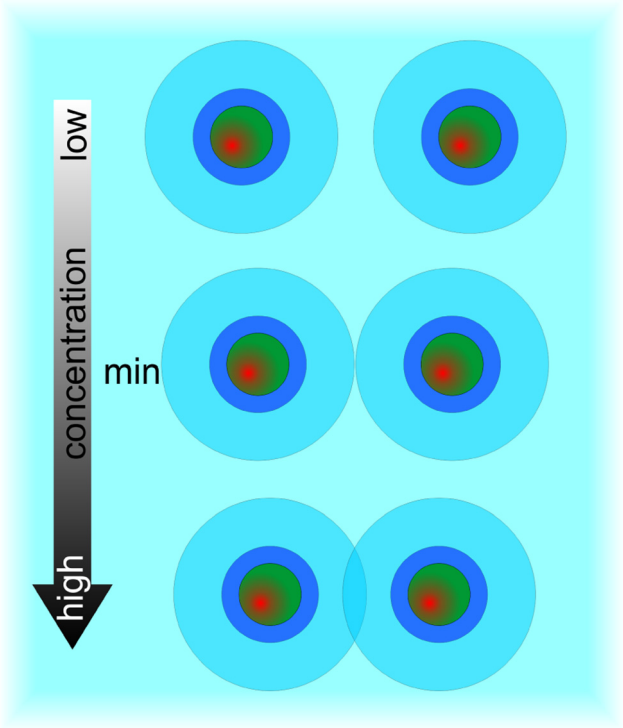

Fig. 5 Hydrated salt molecules overlapping with increasing concentration. The green–red sphere represents the bare salt molecule, after adding the blue shell of strongly attached water molecules we get the salt particle (HSP), while after adding next the outer light blue shell of perturbed water we arrive at the hydrated salt molecule, called FHP. At concentrations above m_{min} the outer shells overlap as shown in the bottom row.

is called the molarity, the number of moles of salt per liter of solution. V_{HS} is the volume of one FHP, *i.e.* one hydrated salt molecule or anion, N_s is the number of salt molecules in volume V, and ρ is the density of the solution. With m_{min}= 1.0 mol kg^{-1} for all systems and a random close packed volume fraction ϕ_{rcp} = 0.64, we obtain R_{HS} = 6.3 Å; this is a very reasonable value according to Mitev *et al.*[47]

On increasing the concentration beyond m_{min}, the outer hydration shells of the salt molecules begin to overlap, as shown in Fig. 5. This gives rise to a type of depletion interaction between the salt molecules, which we will now explain. First we notice that concentrations are never large enough for the tightly bound water molecules, constituting the first solvation layer, of two different salt molecules or anions to touch. Therefore we take HSPs as the coarse grain particles in our model. Similarly we define coarse water particles to consist of several water molecules. The energy of a salt solution is then written as

$$E = \sum_{i=1}^{N_s-1}\sum_{j=i+1}^{N_s}\phi_{ss}^{0}(r_{ij}) + \sum_{i=1}^{N_w-1}\sum_{j=i+1}^{N_w}\phi_{ww}(r_{ij}) + \sum_{i=1}^{N_s}\sum_{j=1}^{N_w}\phi_{sw}(r_{ij}) + E^{self}. \quad (4)$$

Here ϕ_{ss}^{0} denotes the interaction potential between two coarse salt particles, *i.e.* two HSPs at a distance r_{ij}, ϕ_{ww} that between two coarse water particles and ϕ_{sw} that between an HSP and a coarse water particle. E^{self} is an additional self energy depending on the configuration of all HSPs collectively, which is the key quantity in our model.

When one molecule of salt is dissolved in water, the change of energy has two contributions, one negative contribution when the first layer of water molecules is bound to the salt, and one positive contribution that takes into account the perturbation of the outer hydration shell. The total increase of energy will be negative. At low concentrations, when the FHPs do not overlap, a total energy E^0 proportional to the number of salt particles will be released. When two FHPs do overlap, the energies gained by attaching the strongly bound water shells to each of the bare salt molecules, *i.e.* by creating the HSPs, are the same as for two non-overlapping FHPs, but the energy paid to create the outer shells of the FHPs is diminished by a positive amount, proportional to the overlap of the two outer shells. This holds for any pair of overlapping hydration shells. The self energy therefore reads

$$\begin{aligned} E^{self} &= E^0 - \sum_{i<j}^{N_s}\kappa\frac{1}{4}H_{ij}^2(3-H_{ij}) \quad H_{ij}\geq 0 \quad (r_{ij}\leq 2R_{HS}) \\ &= 0 \qquad\qquad\qquad\qquad\quad H_{ij}\leq 0 \quad (r_{ij}\geq 2R_{HS}) \end{aligned} \quad (5a,b)$$

where $H_{ij} = 1 - r_{ij}/2R_{HS}$ is half the thickness of the overlap, divided by R_{HS}, and κ is a positive constant with the dimensions of energy. With this we get for the total energy of the solution

$$E = \sum_{i=1}^{N_s-1}\sum_{j=i+1}^{N_s}\phi_{ss}^{total}(r_{ij}) + \sum_{i=1}^{N_w-1}\sum_{j=i+1}^{N_w}\phi_{ww}(r_{ij}) + \sum_{i=1}^{N_s}\sum_{j=1}^{N_w}\phi_{sw}(r_{ij}), \quad (6a)$$

$$\phi_{ss}^{total}(r_{ij}) = \phi_{ss}^{0}(r_{ij}) - \kappa\frac{1}{4}H_{ij}^2(3-H_{ij}) =: \phi_{ss}^{0}(r_{ij}) + \phi_{ss}^{overlap}(r_{ij}) \quad (6b)$$

where we have omitted the unimportant constant E^0. Evidently, with increasing concentrations the assumed pairwise-additivity of the correction to the self-energy becomes inaccurate.

On the energy scales that we are interested in, coarse salt particles may be considered to be impenetrable particles interacting through dipole–dipole interactions, so ϕ_{ss}^{0} may well be approximated by a Lennard-Jones potential. Given the dimensions as shown in Fig. 1 the radius of a coarse salt particle is about one half of R_{HS}, so the salt–salt Lennard-Jones potential has a σ of about R_{HS}, and therefore a range of about $2\sigma = 2R_{HS}$, which is equal to that of the overlap potential $\phi_{ss}^{overlap}$. For computational purposes it is often most convenient to have water particles of about the same size as that of the salt particle. Clearly for coarse water–water and salt–water interactions somewhat more soft potentials seem to be preferable, although Lennard-Jones potentials have been used for this purpose as well. For a review see Hadley and McCabe.[55] This concludes the description of our coarse grain picture of salt solutions at low concentrations.

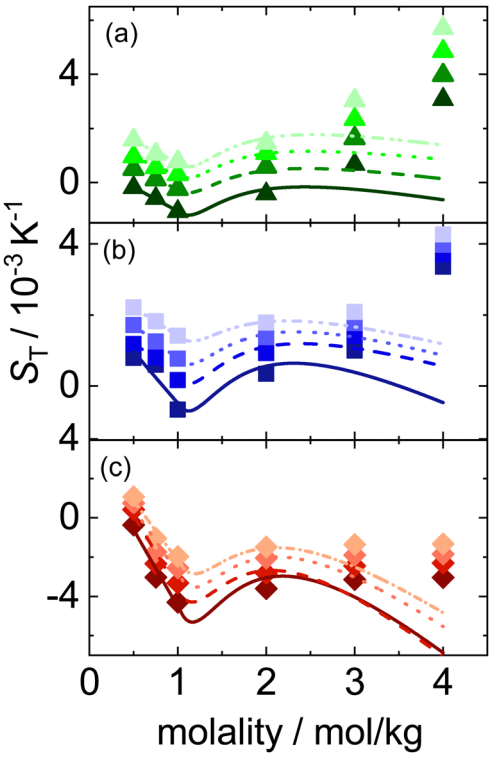

Fig. 6 Concentration dependence of Soret coefficient S_T of KI (upper panel), NaI (middle panel) and LiI (lower panel) at four different temperatures. In each panel temperatures are 15, 25, 35 and 45 °C in that order, with the lowest temperature corresponding to the darkest set of symbols. Lines correspond to fits that have been obtained with our model (for details see Section 3.1).

3.1.2 Estimated predictions. In order to test the validity of this model one has to perform simulations or try to extract information otherwise. Here we will present the results of some rather sketchy calculations on the basis of the results published by Artola and Rousseau for Lennard-Jones mixtures. To this end we assume Lennard-Jones potentials for coarse water–water and salt–water interactions and map the total coarse salt–salt potential $\phi_{ss}^{total}(r_{ij}) = \phi_{ss}^{0}(r_{ij}) + \phi_{ss}^{overlap}(r_{ij})$ on some effective Lennard-Jones potential ϕ_{ss}^{eff}. With these we next make use of the reported data in the paper of Artola and Rousseau. Details of the calculations are presented in the Appendix to this paper. Evidently, mapping the sum of $\phi_{ss}^{0}(r_{ij})$ and $\phi^{overlap}(r_{ij})$, with rather different distance dependencies, to an effective Lennard-Jones potential, must be approximate. We assume, however, that for concentrations not too far above m_{min} the approximation works acceptably. The results obtained with this method must be considered as a proof of principle. The final verdict has to be given by means of a simulation study. Until then, the model remains somewhat speculative, although intuitively appealing.

The results of our calculations are shown as the lines in Fig. 6. It is clearly seen that the predicted Soret coefficients increase as soon as the outer hydration shells of the big spheres begin to overlap. At larger concentrations, however, they decay again while experimental data continue to increase. Apart from the numerical inadequacies already mentioned, also the model itself will become inadequate at the larger concentrations. First, the pairwise additive corrections to the self energies will become inappropriate, and next, at even higher concentrations, one can imagine that it is profitable to form clusters of salt particles and expel the water molecules from these altogether to minimize the energy stored in the perturbed hydration shells. Both effects will lower the average salt–salt interactions faster than is done within the present model, and will drive salt to the cold.

3.2 Temperature dependence

As can be seen in Fig. 4 S_T of all investigated systems shows an increase in thermophobicity with temperature and can be successfully described by eqn (2) for all concentrations studied. The same behavior has been recently observed for other simple salts without large organic groups,[38,56] which is in contrast to the temperature dependence of S_T observed for larger organic salts[37,57] and non-ionic solutes in water.[29] For a typical non-ionic solute, the behavior of S_T changes from increasing with temperature to decreasing with temperature as the concentration increases. It is assumed that this is correlated with the hydration of the solutes, which decreases as the concentration increases. In contrast, the Soret coefficients of simple ionic solutes show the typical temperature dependence described by eqn (2) over the entire concentration range. This might be explained by cluster formation and growth of the salts with increasing concentrations. At high salt concentrations, these clusters are hydrated by water as the fraction of ions in the interfaces decreases when more ions are part of larger clusters. This results in diluted solutions of clusters, which still exhibit the typical temperature dependence of diluted aqueous solutions.

4 Conclusion

We have studied the thermophoretic properties of three iodide salt solutions over a range of temperatures and concentrations. For all three salts, LiI, NaI and KI, the variation of the Soret coefficient with concentration exhibits a minimum for all four temperatures that we investigated. On the basis of various theoretical expressions combined with the best thermodynamic enthalpies and activity coefficients available, we were not able to describe this minimum. On the contrary, in most cases we predicted a maximum in Soret coefficient with concentration.

All experimental data share the same characteristics. First, Soret coefficients at low concentrations decay linearly with concentration, and second, in all cases a minimum occurs at one and the same concentration of one mole of salt per kilogram of solvent. From this we infer that the relevant objects in all systems are to a large extent equally big and behave like ideally dissolved particles at low concentrations. From the concentration where the minimum occurs we obtain an estimate for the size of these objects, which coincides with that of a salt molecule including the full hydration shell of strongly

attached and perturbed water molecules. Beyond the concentration where the Soret coefficient is minimal, the hydrated objects begin to overlap which leads to stronger interactions between salt molecules, much like depletion interactions do in colloid–polymer solutions. Preliminary, somewhat sketchy calculations indicate that indeed the Soret coefficient increases when concentrations increase beyond one mole of salt per kilogram of water. The model only holds at concentrations not very much larger than close packing of the big hydrated objects. At even larger concentrations the pair wise approximation on which the model is built may not be accurate enough. Moreover at large concentrations it may be energetically profitable for the system to expel the water between the salt molecules and form salt clusters.

Conflicts of interest

There are no conflicts to declare.

Appendix

In this appendix we describe how we map our model on the binary Lennard-Jones model of Artola and Rousseau in order to be able to make use of their numerical data on S_T for these systems. We summarize the data of these authors as

$$S_T(x) = -\frac{1}{140}[k-1][x-x_0], \tag{7a}$$

$$x_0 = 0.635\frac{1}{\psi} - 0.142, \tag{7b}$$

where x is the mole fraction of A-particles and k and ψ are set parameters. Their relation to the Lennard-Jones potential parameters is according to $\varepsilon_{AB} = k\sqrt{\varepsilon_{AA}\varepsilon_{BB}}$ and $\psi = \varepsilon_{BB}/\varepsilon_{AA}$. The values of x_0 are obtained from the simulations and have been fitted by us as in eqn (7b).

As noticed in the main text, the radius of the bare salt molecule plus the attached water layer is about half the radius of the fully hydrated salt molecule. Moreover, our concentrations will never be large enough that the attached water layers become perturbed as well. Given these two facts, we consider one salt molecule together with Z attached water molecules to be one LJ_s particle of diameter σ equal to R_{HS}. A LJ_w particle then consists of $Z + \alpha$ water molecules, such that it has the same diameter and preferably the same mass as the salt particles. With this we calculate the Lennard-Jones mole-fractions for salt according to

$$x = \frac{N_s}{N_s + \dfrac{N_w - ZN_s}{Z+\alpha}} = (Z+\alpha)\frac{m}{m_0 + \alpha m}. \tag{8}$$

Since there is no definite way to decide about the size of a particle of $Z + \alpha$ water molecules we settle for $\alpha = 1$. All Lennard-Jones potentials have the same value for σ, which plays no further role in what follows.

We now must decide about the values of k and ψ. These are determined by the three epsilon values $\varepsilon_{AA} = \varepsilon_{ss}^{eff}$, $\varepsilon_{BB} = \varepsilon_{ww}$ and $\varepsilon_{AB} = \varepsilon_{sw}$, of which ε_{ww} and ε_{sw} remain constant throughout this appendix. Moreover only values of $\varepsilon_{ss}^{eff}/\varepsilon_{ww}$ are needed explicitly. First, we determine $\varepsilon_{ss}^{0}/\varepsilon_{ww} = 1/\psi^0$ by putting the overlap potential to zero for molalities less than m_{min}. By fitting the experimental data in this range with eqn (7) we get k^0 and ψ^0 for the zeroth order potentials. For molalities larger than m_{min} we assume that the total salt–salt potential, $\phi_{ss}^{total}(r_{ij})$ may be approximated by the effective Lennard-Jones potential

$$\phi_{ss}^{eff}(r_{ij}) = \phi_{ss}^{0}(r_{ij}) + \frac{\phi_{ss}^{overlap}(r^{NN})}{\phi_{ss}^{0}(r^{NN})}\phi_{ss}^{0}(r_{ij}), \tag{9}$$

where r^{NN} is the average nearest neighbor distance between salt molecules. This gives rise to an effective ε^{eff} given as

$$\varepsilon_{ss}^{eff} = \varepsilon_{ss}^{0} + \kappa\frac{\tilde{\phi}_{ss}^{overlap}(r^{NN})}{\tilde{\phi}_{ss}^{0}(r^{NN})}, \tag{10}$$

where the tildes indicate that factors bearing the dimensions of energy have been taken out, *i.e.* $\tilde{\phi}_{ss}^{0} = \phi_{ss}^{0}/\varepsilon^0 = \phi^{LJ}/\varepsilon$, *etc*. Since both the numerator and the denominator in the last term are negative, the effective epsilon is larger than the pure epsilon, so binding becomes stronger. In order to complete the calculation of k and ψ as function of concentration we must relate r^{NN} to the concentration. To this end we approximate

$$r^{NN}(\mathscr{M}) = 1 + \left(\frac{\mathscr{M}_{min}}{\mathscr{M}}\right)^{1/3}. \tag{11}$$

For $\mathscr{M} = \mathscr{M}_{min}$ we get $r^{NN} = 2$, and for very large concentrations $r^{NN} = 1$.

We now have available all information to calculate k and ψ as functions of concentration:

$$\frac{1}{\psi(\mathscr{M})} = \frac{1}{\psi^0} + \Lambda\frac{\tilde{\phi}_{ss}^{overlap}(r^{NN}(\mathscr{M}))}{\tilde{\phi}_{ss}^{0}(r^{NN}(\mathscr{M}))}, \tag{12a}$$

$$k(\mathscr{M}) = k^0\sqrt{\psi(\mathscr{M})/\psi^0}, \tag{12b}$$

where $\Lambda = \kappa/\varepsilon_{ww}$ is an adjustable parameter. Putting these values into eqn (7) we calculate S_T for any concentration.

Acknowledgements

We thank Fernando Bresme, Julia Burkhardt, Niels Hansen, Jutta Luettmer-Strathmann, Daniel Markthaler, Gunwoo Park, Annette Schmidt and Nils Zimmermann for fruitful and helpful discussions. We are grateful to Jan Dhont and Peter Lang for inspiring ideas and his generous support of our work. SM acknowledges the support of the International Helmholtz Research School of Biophysics and Soft Matter (BioSoft).

References

1 M. Jerabek-Willemsen, T. Andre, R. Wanner, H. M. Roth, S. Duhr, P. Baaske and D. Breitsprecher, *J. Mol. Struct.*, 2014, **1077**, 101–113.
2 D. Niether, M. Sarter, B. W. Koenig, J. Fitter, A. M. Stadler and S. Wiegand, *Polymers*, 2020, **12**, 376.
3 B. T. Huang, M. Roger, M. Bonetti, T. J. Salez, C. Wiertel-Gasquet, E. Dubois, R. Cabreira Gomes, G. Demouchy, G. Mériguet, V. Peyre, M. Kouyaté, C. L. Filomeno, J. Depeyrot, F. A. Tourinho, R. Perzynski and S. Nakamae, *J. Chem. Phys.*, 2015, **143**, 054902.
4 M. Jokinen, J. A. Manzanares, K. Kontturi and L. Murtomäki, *J. Membr. Sci.*, 2016, **499**, 234–244.
5 N. Jaziri, A. Boughamoura, J. Mueller, B. Mezghani, F. Tounsi and M. Ismail, *Energy Rep.*, 2020, **6**, 264–287.
6 F. Hofmeister, *Arch. Exp. Pathol. Pharmakol.*, 1888, **24**, 247–260.
7 Y. Zhang and P. S. Cremer, *Curr. Opin. Chem. Biol.*, 2006, **10**, 658–663.
8 W. Kunz, *Specific ion effects*, World Scientific, Singapore and Hackensack NJ, 2010.
9 *Thermal nonequilibrium phenomena in fluid mixtures*, ed. W. Köhler and S. Wiegand, Springer, Berlin, 1st edn, 2002, vol. LNP584.
10 D. Niether and S. Wiegand, *J. Phys.: Condens. Matter*, 2019, **31**, 503003.
11 C. C. Tanner, *Trans. Faraday Soc.*, 1927, **23**, 75–95.
12 J. Chanu, *J. Chim. Phys. Phys.-Chim. Biol.*, 1958, **55**, 743–753.
13 J. Chanu, in *Advances in Chemical Physics*, ed. I. Prigogine, John Wiley & Sons, Inc, Hoboken, NJ, USA, 1967, pp. 349–367.
14 F. S. Gaeta, G. Perna, G. Scala and F. Bellucci, *J. Phys. Chem.*, 1982, **86**, 2967–2974.
15 J. Colombani, J. Bert and J. Dupuy-Philon, *J. Chem. Phys.*, 1999, **110**, 8622–8627.
16 S. Di Lecce, T. Albrecht and F. Bresme, *Phys. Chem. Chem. Phys.*, 2017, **19**, 9575–9583.
17 I. Prigogine, L. Debrouckere and R. Amand, *Physica*, 1950, **16**, 851–860.
18 P. Polyakov and S. Wiegand, *J. Chem. Phys.*, 2008, **128**, 034505.
19 Z. Wang, H. Kriegs and S. Wiegand, *J. Phys. Chem. B*, 2012, **116**, 7463–7469.
20 S. R. de Groot, *Thermodynamics of irreversible processes*, North Holland, Amsterdam, 1966.
21 R. Haase, *Thermodynamik der Irreversiblen Prozesse*, Steinkopff, Heidelberg, 1963, vol. 8.
22 S. Kjelstrup, D. Bedeaux, E. Johannessen and J. Gross, *Non-equilibrium thermodynamics for engineers*, World Scientific, Hackensack, NJ, 2nd edn, 2017.
23 K. Shukla and A. Firoozabadi, *Ind. Eng. Chem. Res.*, 1998, **37**, 3331–3342.
24 L. J. T. M. Kempers, *J. Chem. Phys.*, 2001, **115**, 6330–6341.
25 M. G. Gonzalez-Bagnoli, A. A. Shapiro and E. H. Stenby, *Philos. Mag.*, 2003, **83**, 2171–2183.
26 M. Hartung and W. Köhler, *Eur. Phys. J. E: Soft Matter Biol. Phys.*, 2009, **29**, 117–121.
27 A. Königer, B. Meier and W. Köhler, *Philos. Mag.*, 2009, **89**, 907–923.
28 P. Blanco, H. Kriegs, B. Arlt and S. Wiegand, *J. Phys. Chem. B*, 2010, **114**, 10740–10747.
29 D. Niether, H. Kriegs, J. K. G. Dhont and S. Wiegand, *J. Chem. Phys.*, 2018, **149**, 044506.
30 D. Vigolo, S. Buzzaccaro and R. Piazza, *Langmuir*, 2010, **26**, 7792–7801.
31 D. Lide, T. J. Bruno and J. R. Rumble, *CRC handbook of chemistry and physics: A ready-reference book of chemical and physical data*, 100th edn, 2019.
32 R. Heyrovská, *Chem. Phys. Lett.*, 1989, **163**, 207–211.
33 J. A. Myers, S. I. Sandler and R. H. Wood, *Ind. Eng. Chem. Res.*, 2002, **41**, 3282–3297.
34 S. Iacopini, R. Rusconi and R. Piazza, *Eur. Phys. J. E: Soft Matter Biol. Phys.*, 2006, **19**, 59–67.
35 Y. Kishikawa, S. Wiegand and R. Kita, *Biomacromolecules*, 2010, **11**, 740–747.
36 D. Niether, D. Afanasenkau, J. K. G. Dhont and S. Wiegand, *Proc. Natl. Acad. Sci. U. S. A.*, 2016, **113**, 4272–4277.
37 A. L. Sehnem, D. Niether, S. Wiegand and A. M. F. Neto, *J. Phys. Chem. B*, 2018, **122**, 4093–4100.
38 S. Mohanakumar, J. Luettmer-Strathmann and S. Wiegand, *J. Chem. Phys.*, 2021, **154**, 084506.
39 P. A. Artola and B. Rousseau, *Phys. Rev. Lett.*, 2007, **98**, 125901.
40 O. R. Gittus and F. Bresme, On the microscopic origin of Soret coefficient minima in liquid mixtures, **https://arxiv.org/pdf/2207.12864**.
41 H. S. Frank and W.-Y. Wen, *Discuss. Faraday Soc.*, 1957, **24**, 133.
42 M. Carrillo-Tripp, H. Saint-Martin and I. Ortega-Blake, *J. Chem. Phys.*, 2003, **118**, 7062–7073.
43 A. K. Soper and K. Weckström, *Biophys. Chem.*, 2006, **124**, 180–191.
44 R. Mancinelli, A. Botti, F. Bruni, M. A. Ricci and A. K. Soper, *J. Phys. Chem. B*, 2007, **111**, 13570–13577.
45 J. Gujt, M. Bešter-Rogač and B. Hribar-Lee, *J. Mol. Liq.*, 2014, **190**, 34–41.
46 P. Gallo, D. Corradini and M. Rovere, *J. Mol. Liq.*, 2014, **189**, 52–56.
47 K. Hermansson, P. D. Mitev and W. J. Briels, *J. Phys. Chem. B*, 2021, **125**, 13886–13895.
48 G. D. Scott and D. M. Kilgour, *J. Phys. D: Appl. Phys.*, 1969, **2**, 863–866.
49 D. E. Goldsack and R. Franchetto, *Can. J. Chem.*, 1977, **55**, 1062–1072.
50 D. R. Caldwell, *J. Phys. Chem.*, 1975, **79**, 1882–1884.
51 P. N. Snowdon and J. C. R. Turner, *Trans. Faraday Soc.*, 1960, **56**, 1409–1418.
52 R. Heyrovska, *Croat. Chem. Acta*, 1997, **70**, 39–54.
53 I. S. Joung and T. E. Cheatham, *J. Phys. Chem. B*, 2009, **113**, 13279–13290.
54 A. K. Borkowski, Z. A. Piskulich and W. H. Thompson, *J. Phys. Chem. B*, 2021, **125**, 350–359.
55 K. R. Hadley and C. McCabe, *Mol. Simul.*, 2012, **38**, 671–681.
56 S. Mohanakumar and S. Wiegand, *Eur. Phys. J. E: Soft Matter Biol. Phys.*, 2022, **45**, 10.
57 A. L. Sehnem, A. M. F. Neto, R. Aquino, A. F. C. Campos, F. A. Tourinho and J. Depeyrot, *Phys. Rev. E: Stat., Nonlinear, Soft Matter Phys.*, 2015, **92**, 042311.